

DESIGN OF A POLARIZATION-INDEPENDENT MMI SOI COUPLER BASED MICRORESONATOR USING SANDWICH STRUCTURES

TRUNG-THANH LE

Hanoi University of Natural Resources and Environment,
No. 41A, K1 Road, Phu Dien, Tu Liem, Hanoi, Vietnam
E-mail: thanh.le@hunre.edu.vn

Abstract

A microresonator based on multimode interference (MMI) couplers using sandwich structures is described in this paper. The birefringence can be controlled by introducing an additional dielectric layer within a silicon channel waveguide. It is shown that a polarization-independent MMI coupler based ring resonator can be achieved by choosing appropriate structure parameters.

Keywords: Multimode interference (MMI) coupler, Silicon-on-insulator (SOI), Microresonator.

1. Introduction

Silicon-on-insulator (SOI) waveguides are attractive platforms for constructing various micro-optic optical devices and photonic integrated circuits that can be used for future photonic network systems. Due to their small bending radius, silicon wires [1-3] are attractive for use in small footprint photonic applications. Many functional optical devices have been demonstrated with these waveguide structures, such as channel-dropping filters with small waveguides, ring resonators, optical modulators, optical filters, and optical switches with high performance [4, 5]. However, due to the high index contrast between Si and SiO₂, optical devices based on these structures can be extremely polarization-dependent.

Ring resonators are promising candidates for photonic signal processing applications such as wavelength filtering, routing, switching, modulation, and multiplexing applications. Ring resonators have been reported using directional couplers or 2×2 multimode interference (MMI) couplers as the coupling element between the ring and the bus waveguides. A ring resonator based on polarization-

Nomenclatures

h	Height of the waveguide channel (Fig. 1), μm
h_s	Thickness of the sandwich region (Fig. 1), μm
L_{MMI}	Length of the MMI coupler, μm
L_R	Racetrack circumferences (Fig. 6), μm
L_π	The beat length of an MMI coupler, μm
n_{eff}	Effective refractive index
n_s	Refractive index of the sandwich region
n_1	Refractive index of silica cladding, $n_1 = 1.45$
n_2	Refractive index of silicon core, $n_2 = 3.5$
R	Radius of the ring waveguide, μm
T	Transmission
W	Width of the optical waveguide channel, μm

Greek Symbols

α	Loss factor of the waveguide, dB/cm
β	Propagation constant of the ring waveguide
β_o	Propagation constant of the lowest order mode
β_1	Propagation constant of the second lowest order mode
ΔL_π	The difference in beat lengths of the two polarizations, μm
ϕ	Phase accumulated over the ring waveguide
λ	Optical wavelength, μm

Abbreviations

MMI	Multimode interference
SOI	Silicon on insulator

independent directional couplers using the silicon-on-insulator (SOI) platform has been reported [6-8], where the directional coupler length was designed to produce the same coupling ratio for both TE and TM polarized light.

Moreover, MMI structures have been widely used in a number of communication applications and have become a basic building block for many optical devices, due to the advantages of relaxed fabrication tolerances, ease of integration of these devices into more complex photonic integrated circuits, small size, and low excess loss [9]. Therefore, the MMI coupler is a good candidate for the coupling element in a ring resonator, instead of a directional coupler.

An approach to obtaining a polarization-independent ring resonator based on MMI couplers by using stress engineering is given in by Xu et al. [10, 11]. However, the drawback of this method is that the polarization-independent control range is quite small [10]. There have been some other methods presented for the design of directional coupler based polarization-independent microring resonator structures on silicon-on-insulator (SOI) [12] and on GaAs/AlGaAs [13]. An approach to the design of a polarization-insensitive MMI coupler based microring resonators on InGaAsP/InP has been reported [14, 15]. In these reported methods, by choosing the appropriate waveguide structure parameters, polarization-independent microring resonators have been achieved.

For SOI platform based waveguides, an alternative approach to birefringence control is to introduce an additional dielectric layer into a channel waveguide structure, similar to that proposed for slab waveguide structures [16]. Based on this approach, a 1×2 ultra-small size MMI coupler using a channel structure on SOI has been obtained [17] and a formula for the design of polarization-insensitive multimode interference couplers has also been reported [18]. The structure is based on silicon photonic wires with a lower refractive index between silicon layers [19]. However, the design of single mode and polarization-independent waveguides, combined with polarization-independent 2×2 MMI couplers are critical issues that need to be considered in detail. Moreover, a polarization-insensitive MMI based microring resonator on silicon channel waveguides has not previously been reported, to the authors' knowledge.

In this paper, we design and analyse a ring resonator based on a 2×2 MMI coupler using sandwich structures for birefringence control. The MMI coupler and waveguide parameters are optimized to allow the designer to be able to achieve waveguides and MMI based microring resonators that are all polarization-independent. All the simulations for this paper have used numerical schemes based on the 3D eigenmode-expansion method (EME) [20].

2. Single Mode and Polarization-Independent Waveguide

In order to obtain a polarization-independent microring resonator, the access waveguides at input and output ports of the MMI coupler must meet the single mode requirement and be polarization-independent waveguides.

We consider a channel waveguide as shown in Fig. 1. The structure of the channel waveguide comprises three layers: the upper and lower layers are Si, whilst the middle layer has a lower refractive index than Si. This sandwich or intermediate layer can be polymer material or SiN which has a controllable refractive index. The sandwich layer has thickness h_s and refractive index n_s . The width of the waveguide is W and is and the etched depth is h , which is the same as the total channel height. In this study, the waveguide parameters used for this structure are as follows: the refractive index of the Si core, $n_2 = 3.5$ and the SiO_2 cladding, $n_1 = 1.45$.

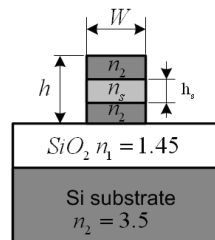


Fig. 1. Geometry of a Channel Waveguide Having a Sandwich Structure.

This sandwich waveguide structure, sometimes called a slot waveguide [17], supports hybrid modes which can be approximated by quasi TE (transverse electric) and quasi TM (transverse magnetic) modes. The electric fields of the quasi TM modes are largely confined to the low index intermediate layer due to the electric field discontinuities at the interfaces. In contrast, the electric fields of the quasi TE modes are more generally distributed across the waveguide. By

judicious choice of the dimensions and the refractive indices, it is possible to design a waveguide such that the propagation constants of the fundamental quasi TM and quasi TE modes are identical.

The first step in the design of the channel waveguide is to identify the range of parameters that will guarantee single mode operation. The waveguide width requirements for single mode operation were obtained using the eigenmode-expansion method (EME). The simulations were carried out for channel waveguides with a height of $h = 500$ nm, and a thickness of the sandwich region $h_s = 100$ nm. The results are illustrated in Fig. 2. In order to achieve single mode operation, the single mode requirements for both quasi TE and quasi TM modes need to be met simultaneously. Figure 2 shows that for single mode operation, the channel waveguide parameters should lie within the shaded region.

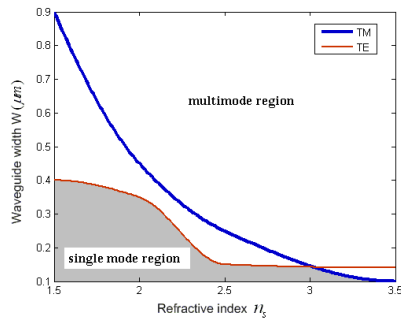


Fig. 2. Single Mode Condition of the Channel Waveguide for Both TE and TM Polarized Light.

After the parameters for meeting the single mode condition have been obtained, the next step is to determine the waveguide parameters to ensure that the waveguides are also polarization-independent. The calculated effective indices of the quasi TE and quasi TM modes of the sandwich channel waveguide are plotted as a function of the channel width in Fig. 3. The waveguide parameters for Fig. 3 are optical wavelength $\lambda = 1.55$ μm and channel waveguide total height $h = 500$ nm. The sandwich region has thickness $h_s = 100$ nm and refractive index $n_s = 1.578$.

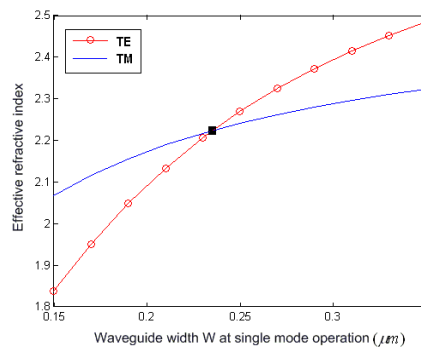


Fig. 3. Calculated Effective Indices for Quasi TE and Quasi TM Modes as a Function of Channel Width.

It is desired to determine the width where the effective indices become equal. Therefore, for a polarization-independent ring resonator, the width of the underlying waveguide must have this value. Here we have kept the waveguide height constant to reduce the leakage loss for the fundamental mode. It can be seen from Fig. 3 that the channel width should be approximately 240 to 250 nm at $n_s = 1.578$ to obtain polarization-independent operation. Although the resulting waveguide has a high height-to-width ratio, computer simulations show that it is indeed single-mode.

3. Polarization-Independent MMI Couplers

We shall now consider similar, but wider, waveguide structures for the MMI region of the device. The length of an MMI coupler is usually a multiple or sub-multiple of a beat length parameter L_π . This beat length can be determined by using the self-imaging theory and is defined as [8]

$$L_\pi = \frac{\pi}{\beta_0 - \beta_1} \quad (1)$$

Here β_0 and β_1 are the propagation constants for the two lowest order modes and they can be calculated by the EME method. For a polarization-insensitive MMI coupler, the difference in beat lengths of the two polarizations should be zero, i.e., $\Delta L_\pi = L_{\pi(\text{TE})} - L_{\pi(\text{TM})} = 0$, where the subscripts in brackets represent the appropriate polarizations.

The next step is to compute the beat lengths for both quasi TE and quasi TM modes as a function of the intermediate layer refractive index for a range of useful channel widths. The aim of these calculations is to find the parameters that will lead to polarization-insensitive MMI structures. To simplify the calculations, we shall keep the height of the channel waveguide constant at $h = 500$ nm. Figures 4(a)-(d) show the results of these EME calculations for a variety of channel widths.

The simulations show that for certain values of the intermediate layer refractive index n_s , polarization-independent MMI couplers can be obtained. The values of L_π and n_s at this point are 25 μm and 1.578 for $W = 3$ μm , 68 μm and 1.732 for $W = 5$ μm , 278 μm and 2.2 for $W = 10$ μm . When the width of the MMI region is increased to greater than around 70 μm , there is no crossing of the L_π curve of the TE mode with the L_π curve of the TM mode, thus polarization-insensitive MMI couplers can no longer be attained. Whilst wide MMI devices may accommodate a large number of ports, these calculations show that for the structures considered here, a width of about 70 μm is the upper limit for polarization-insensitive operation. However, this width would be enough for most applications using integrated optics.

Next, we consider the behavior of the MMI characteristics when the channel height h is varied whilst the refractive index and the width of the sandwich region are held constant at $n_s = 1.578$ and $h_s = 100$ nm, respectively. Figure 5 shows the difference ΔL_π as the MMI width increases for different channel heights. From this figure, one can obtain an optimal width to make $\Delta L_\pi = 0$ for a given channel height. The results again show that typical waveguide heights should be large enough to produce polarization-independent MMI couplers. It must be

remembered that another factor related to the height and width of the MMI region is the required distance between two adjacent access waveguides (larger than about 1 μm) so that the power coupling between the access guides is minimized.

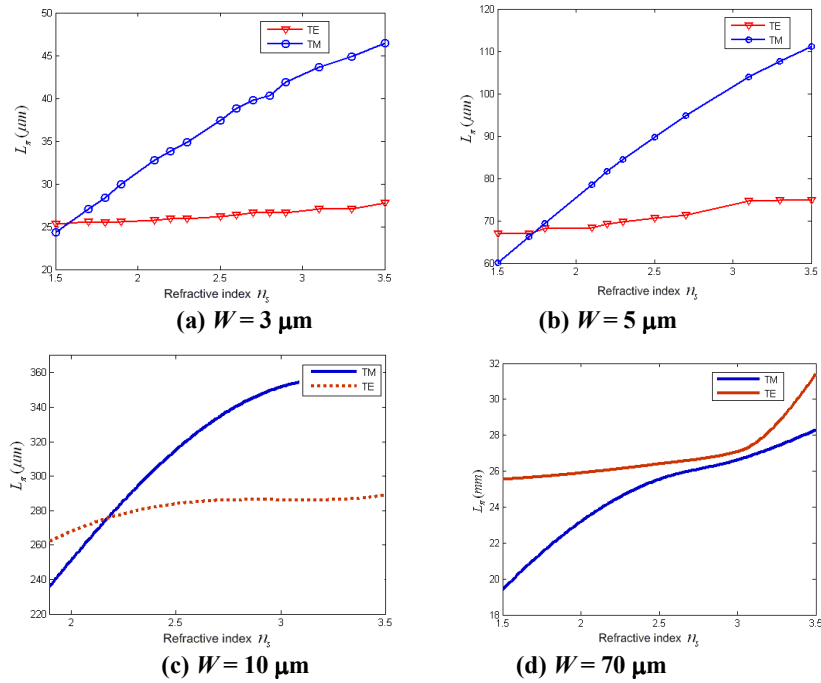


Fig. 4. MMI Beat Length L_{π} as a Function of Refractive Index n_s for an MMI Width of (a) $W = 3 \mu\text{m}$, (b) $W = 5 \mu\text{m}$, (c) $W = 10 \mu\text{m}$, and (d) $W = 70 \mu\text{m}$.

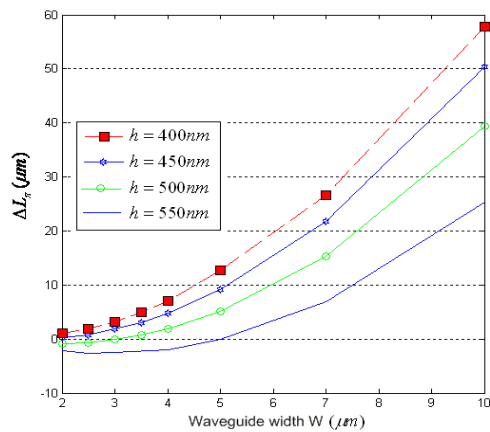


Fig. 5. The Variation of Beat Length Difference ΔL_{π} with MMI Width and Channel Height.

4. Polarization-Independent Ring Resonators Based on MMI Couplers

In this section, a ring resonator based on the above analysis is designed and simulated. The final design aim is to choose the appropriate waveguide and structure parameters to achieve polarization-independent operation for the overall device. To have a small device size, we choose the width of the 2×2 MMI coupler to be $W = 3 \mu\text{m}$, and the height of the waveguide $h = 500 \text{ nm}$. This still guarantees little coupling between the access waveguides. From section 3, we see that to have a polarization-independent MMI coupler, the refractive index of the sandwich region must be about 1.578 and therefore, from Fig. 3 the width of the access waveguides should be about 250 nm. Moreover, by using external effects such as thermo-optic and electro-optic effect on the material of the intermediate layer or by employing the plasma free carrier effect, the characteristics of the channel waveguide can be controlled. In addition, minimizing the sidewall roughness by oxidation techniques for the sidewalls of the waveguide can be applied to reduce the propagation loss [21]. By using this approach, a very small waveguide having a loss of only 0.8dB/cm has been achieved.

The structure of the microring resonator using an MMI coupler is shown in Fig. 6. The 3dB 2×2 MMI coupler was used in this design.

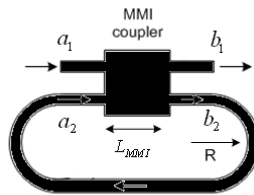


Fig. 6. Ring Resonator Based on the above Analysis.

The MMI coupler is based on the paired interference theory in order to keep the overall size small. The approximate length of MMI coupler can be calculated using self-imaging theory

$$L_{MMI} = \frac{1}{2} p L_{\pi} \quad (2)$$

where p is an integer. For a short device, $p=1$.

The transmission coefficient of an MMI coupler can be calculated using self-imaging theory or by a numerical method such as the Beam Propagation Method (BPM), or the eigenmode-expansion method (EME). Figure 7 shows the simulation results for the transmission coefficients of this MMI coupler at different MMI lengths calculated by using the 3D EME method.

The simulation results show that to obtain a 3dB coupler, the MMI length should be around $11.4 \mu\text{m}$. This length should be compared with the length of $12.5 \mu\text{m}$ calculated by the self-imaging theory from Eq. (2) to achieve a 3dB coupler.

Although a detailed tolerance analysis of the device has not been presented in this paper, it is apparent from the simulation results that the sensitivity to waveguide dimensions would lie within existing fabrication limits. For example,

current nanofabrication technology has a tolerance of around 10 nm which would be ample tolerance for the proposed device.

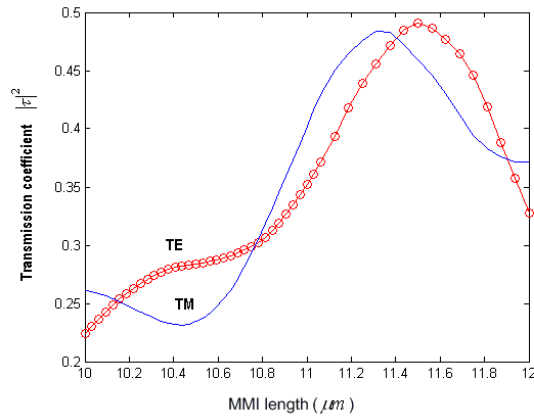


Fig. 7. Transmission Coefficient of the 2×2 MMI Coupler at Different MMI Lengths for the Quasi TE and Quasi TM Modes.

Using the above results, simulations of the field propagation within the MMI region are shown in Figs. 8(a) and (b) for the quasi TE and quasi TM modes, respectively at the optimized length of the MMI coupler.

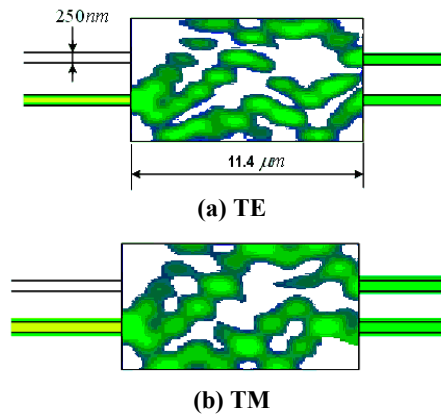


Fig. 8. Electric Field in the MMI Region with a Width 3 μm for Quasi TE and Quasi TM Modes Calculated by EME.

The MMI coupler can be described by a transfer matrix and the relations between the complex amplitudes a_i and b_i at input and output ports can be expressed in terms of a scattering matrix as [22]

$$\begin{pmatrix} b_1 \\ b_2 \end{pmatrix} = \begin{pmatrix} \tau & \kappa \\ -\kappa^* & \tau^* \end{pmatrix} \begin{pmatrix} a_1 \\ a_2 \end{pmatrix} \tag{3}$$

$$a_2 = \alpha e^{i\phi} b_2 \tag{4}$$

where τ , κ are the transmission and coupling coefficients, respectively, of the MMI coupler. Note that $|\kappa|^2 + |\tau|^2 = 1$. The coupler is assumed to be lossless, for simplicity. Light propagation through the resonator is characterized by a round-trip transmission loss $\alpha = \exp(-\alpha_0 L_R)$ and a phase factor $e^{i\varphi}$. The round trip phase is given by $\varphi = 2L_R \pi n_{eff} / \lambda$, where $L_R = L_{MMI} + 2\pi R$ is the racetrack circumferences shown in Fig. 6, and α_0 (dB/cm) is the loss coefficient in the core of the optical waveguide. $\varphi = \beta L_R$ is the phase accumulated over the ring waveguide with propagation constants β , where $\beta = 2\pi n_{eff} / \lambda$. The effective refractive indices of the waveguide core are $n_{eff} = 2.269$ for the TE fundamental mode and $n_{eff} = 2.241$ for the TM fundamental mode. The optical wavelength is denoted by λ .

From Eqs. (3) and (4), the transmission T of the device can be expressed as

$$T = \left| \frac{b_1}{a_1} \right|^2 = \left| \frac{\tau - \alpha e^{i\varphi}}{1 - \tau^* \alpha e^{i\varphi}} \right|^2 \tag{5}$$

Figure 9 shows the general transmission characteristics of a ring resonator designed using the above theory for two cases (a) loss factor $\alpha = 0.8 > |\tau|$, and (b) the critical coupling condition $\alpha = |\tau| = 0.707$. The simulation results show that a polarization-independent ring resonator can be achieved using the design procedure given in this paper.

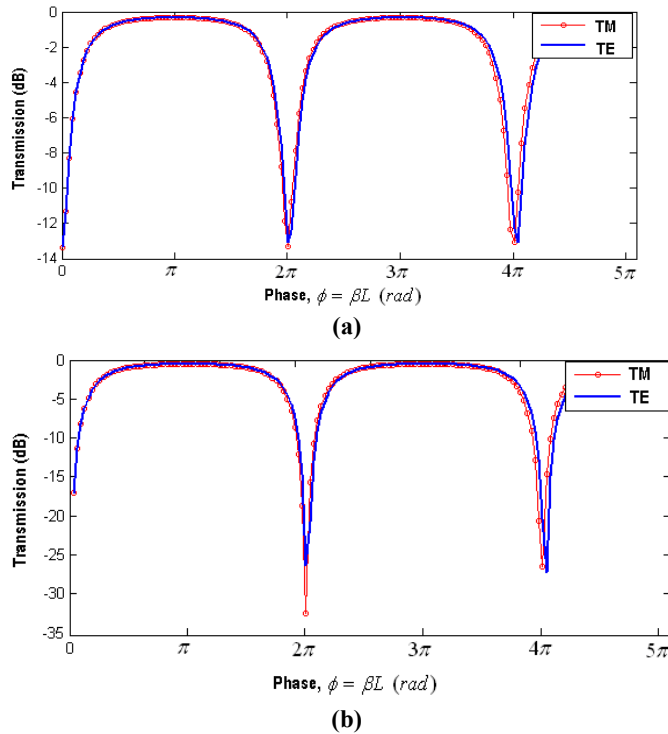


Fig. 9. General Transmission Characteristics of the Device for TE and TM Modes with a Loss Factor (a) $\alpha = 0.8$, and (b) $\alpha = |\tau| = 0.707$, respectively.

5. Conclusions

We have presented a novel approach to the design of polarization-independent optical devices based on MMI couplers. The simulations show that it is possible to use polarization-independent, single mode waveguides and polarization-independent MMI 3dB couplers to make polarization-independent ring resonators. Birefringence control can be obtained by introducing an additional layer into the channel waveguide structure, with this layer having a controllable refractive index. This device can be a basic component for building more complex functional devices having polarization-independent characteristics. For example, these results can be applied to higher order circuits including multiple ring resonators connected in series or parallel to achieve the polarization-independent characteristics.

References

1. Dumon, P.; Bogaerts, W.; and Wiaux, V. (2004). Low-loss SOI photonic wires and ring resonators fabricated with deep UV lithography. *IEEE Photonics Technology Letters*, 16(5), 1328-1330.
2. Janz, S.; Cheben, P.; and Dalacu, D. (2006). Microphotonic elements for integration on the silicon-on-insulator waveguide platform. *IEEE Journal of Selected Topics in Quantum Electronics*, 12(6), 1402-1145.
3. Reed, G.T.; Mashanovich, G.Z.; and Emerson, N.G. (2006). Issues associated with polarization independence in silicon photonics. *IEEE Journal of Selected Topics in Quantum Electronics*, 12(6), 1335-1344.
4. Soref, R. (2006). The past, present, and future of silicon photonics. *IEEE Journal of Selected Topics in Quantum Electronics*, 12(6), 1678-1687.
5. Tsuchizawa, T.; Yamada, K.; Fukuda, H.; Watanabe, T.; Takahashi, J.; Shoji, T.; Tamechika, E.; Itabashi, S.; and Morita, H. (2005) Microphotonic devices based on silicon microfabrication technology. *IEEE Journal of Selected Topics in Quantum Electronics*, 11(1), 232-240.
6. Chan, S.P.; Png, C.E.; Lim, S.T.; Reed, G.T.; and Passaro, V.M.N. (2005). Single-mode and polarization-independent silicon-on-insulator waveguides with small cross section. *IEEE Journal of Lightwave Technology*, 23(6), 2103-2111.
7. Headley, W.R.; Reed, G.T.; and Paniccia, M. (2004) Polarization-independent optical racetrack resonators using rib waveguides on silicon-on-insulator, *Applied Physics Letters*, 85(23), 5523-5525.
8. Chen, X.; and Tsang, K. (2011). Polarization-independent grating couplers for silicon-on-insulator nanophotonic waveguides. *Optics Letters*, 36(6), 796-798.
9. Cahill, L.W. (2003). The synthesis of generalised Mach-Zehnder optical switches based on multimode interference (MMI) couplers. *Optical and Quantum Electronics*, 35(4-5), 465-473.
10. Xu, D.X.; Janz, S.; and Cheben, P. (2006). Design of polarization-insensitive ring resonators in silicon-on-insulator using MMI couplers and cladding stress engineering. *IEEE Photonics Technology Letters*, 18(2), 343-345, 2006.

11. Xu, D.X. (2011). Polarization control in silicon photonic waveguide components using cladding stress engineering. *Topics in Applied Physics*, 119/2011, 31-70.
12. Van Thourhout, D.; Bogaerts, W.; and Dumon, P. (2006). *Optical interconnects: The silicon approach*. Springer, Berlin.
13. Timotijevic, B.D. (2006). Multi-stage racetrack resonator filters in SOI. *Journal of Optics A: Pure and Applied Optics*, 8(7), S473-S476.
14. Chin, M. (2003). Polarization dependence in waveguide-coupled microresonators. *Optics Express*, 11(15), 1724-1730.
15. Chin, M.; Xu, C.; and Huang, W. (2004). Theoretical approach to a polarization-insensitive single-mode microring resonator. *Optics Express*, 12(14), 3245-3250.
16. Aarnio, J.; Heimala, P.; Del Giudice, M.; and Bruno, F. (1991). Birefringence control and dispersion characteristics of silicon oxynitride optical waveguides. *IET Electronics Letters*, 7(25), 2317- 2318.
17. Fujisawa, T. and Koshiba, M. (2006). Theoretical investigation of ultrasmall polarization-insensitive 1×2 multimode interference waveguides based on sandwiched structures. *Photonic Technology Letters*, 18(11), 1246-1248.
18. Chiang, K.S.; and Liu, Q. (2011). Formulae for the design of polarization-insensitive multimode interference couplers. *Photonic Technology Letters*, 23(18), 1277-1279.
19. Almeida, V.R.; Xu, Q.; Barrios, C.A.; and Lipson, M. (2004). Guiding and confining light in void nanostructure. *Optics Letters*, 29(11), 1209-1211.
20. Sudbo, A.S. (1993). Film mode matching: a versatile numerical method for vector mode field calculations in dielectric waveguides. *Pure Applied Optics*, 2(3), 211-233, 1993.
21. Lee, K.K. (2001). *Transmission and routing of optical signals in on-chip waveguides for silicon microphotonics*. Ph.D. thesis, Massachusetts Institute of Technology.
22. Yariv, A. (2000). Universal relations for coupling of optical power between microresonators and dielectric waveguides. *IET Electronics Letters*, 36(4), 321-322.